THE JOURNAL OF BIOLOGICAL CHEMISTRY
Vol. 271, No. 16, Issue of April 19, pp. 9550–9559, 1996
Printed in U.S.A.

The Human Glucocorticoid Receptor β Isoform

EXPRESSION, BIOCHEMICAL PROPERTIES, AND PUTATIVE FUNCTION*

(Received for publication, August 24, 1995, and in revised form, January 23, 1996)

Robert H. Oakley‡§¶, Madhabananda Sar§, and John A. Cidlowski‡**

From the ‡Laboratory of Integrative Biology, National Institute of Environmental Health Sciences, Research Triangle Park, North Carolina 27709 and the §Department of Physiology, University of North Carolina at Chapel Hill, Chapel Hill, North Carolina 27599

Alternative splicing of the human glucocorticoid receptor (hGR) primary transcript produces two receptor isoforms, hGRα and hGRβ, which differ at their carboxyl termini. The hGRα isoform conveys endocrine information to target tissues by altering patterns of gene expression in a hormone-dependent fashion. In contrast to hGRα, very little is known about the hGRβ splice variant. Using hGRα- and hGRβ-specific riboprobes on human multiple tissue Northern blots, we show that the hGRβ message has a widespread tissue distribution. We also prove by reverse transcriptase-polymerase chain reaction that the alternative splicing event underlying the formation of the hGRβ message occurs in these tissues. Because the hGRβ protein differs from hGRα at the extreme COOH terminus, we investigated several of the biochemical properties of hGRβ expressed in transfected cells. hGRβ does not bind the glucocorticoid agonist dexamethasone nor the glucocorticoid antagonist RU38486 *in vivo*. Moreover, in contrast to hGRα, hGRβ is located primarily in the nucleus of transfected cells independent of hormone administration. Finally, in the absence of hGRα, hGRβ is transcriptionally inactive on a glucocorticoid-responsive enhancer. However, when both isoforms are expressed in the same cell, hGRβ inhibits the hormone-induced, hGRα-mediated stimulation of gene expression. Thus, hGRβ potentially functions as a dominant negative inhibitor of hGRα activity.

Two human glucocorticoid receptor (hGR)[1] cDNA clones, termed hGRα and hGRβ, were isolated in 1985 that predicted the existence of two receptor isoforms differing at their carboxyl termini (1). Amino acid sequence analysis revealed that the hGRα and hGRβ isoforms were identical through amino acid 727 but diverged beyond this position with hGRα having an additional 50 amino acids and hGRβ an additional, nonhomologous 15 amino acids. Exons 1–8 of the hGR gene contain the 5′ noncoding and coding sequences common to the hGRα and hGRβ cDNAs, and exons 9α and 9β contain the coding and 3′ noncoding sequences specific to the hGRα and hGRβ cDNAs (2). Because the hGRα- and hGRβ-specific sequences are located on the same gene, alternative splicing of exons 9α and 9β was speculated to be the mechanism responsible for generating the two receptor isoforms. However, initial Western blot analysis detected only the larger 94-kDa hGRα isoform, and only hGRα appeared to bind hormone and induce expression of a glucocorticoid-responsive reporter plasmid in a hormone-dependent manner (1, 3). Because of its predominant expression, ligand binding properties, and transcriptional activity, hGRα became the primary focus of subsequent research. As a result, its expression, biochemical properties, and physiological function have been well characterized.

hGRα is expressed in most human tissues and cell lines and belongs to the superfamily of steroid/thyroid/retinoic acid receptor proteins that function as ligand-dependent transcription factors (for reviews see Refs. 4–6). Members of this family are organized into structurally and functionally defined domains. Specifically, hGRα is comprised of a unique amino-terminal variable region that includes a transactivation domain that is important for regulation of gene expression. hGRα also contains a central DNA-binding domain crucial for specific interaction of the receptor with DNA sequences containing glucocorticoid receptor responsive elements (GRE). The carboxyl terminus of the hGRα protein contains the hormone-binding domain as well as sequences important for interaction with heat shock protein 90 (hsp90) (7), nuclear translocation (8), receptor dimerization (9), and transactivation (10).

In the absence of hormone, hGRα resides predominantly in the cytoplasm of cells, where it exists as a large multiprotein complex (for reviews see Refs. 11 and 12). This complex appears to consist of the receptor polypeptide, two molecules of hsp90, and several additional proteins. The association of hsp90 with the receptor is believed to maintain the receptor in a high affinity hormone binding state and sequester the receptor in the cytoplasm by inactivating the nuclear localization signals (NLS). Once hormone binds the receptor, a conformational change ensues resulting in the dissociation of hsp90 and the other associated proteins. In its new conformation hGRα translocates into the nucleus, where it binds as a homodimer to GREs that are usually found in the promoter regions of steroid-responsive genes. The receptor then communicates with the basal transcription machinery to either enhance or repress transcription of the linked gene. hGRα can also modulate gene expression by physically interacting with other nuclear proteins such as AP-1 (13–15) and NF-κB (16).

In contrast to hGRα, very little is known about the physiological significance of hGRβ. We demonstrate here that a mRNA transcript consistent in size with the hGRβ cDNA is expressed in various human adult and fetal tissues and in

* The costs of publication of this article were defrayed in part by the payment of page charges. This article must therefore be hereby marked "*advertisement*" in accordance with 18 U.S.C. Section 1734 solely to indicate this fact.

¶ Supported in part by a National Science Foundation Graduate Fellowship.

** To whom correspondence should be addressed: National Institute of Environmental Health Sciences, P.O. Box 12233, MD E2-02, Research Triangle Park, NC 27709. Tel.: 919-541-1564. Fax: 919-541-1367.

[1] The abbreviations used are: hGR, human glucocorticoid receptor; GRE, glucocorticoid receptor responsive elements; hsp90, heat shock protein 90; NLS, nuclear localization signal; MMTV, mouse mammary tumor virus; DEX, dexamethasone; RU486, RU38486; CAT, chloramphenicol acetyltransferase; 3′UTR, 3′-untranslated region; TRα, thyroid hormone receptor α; RT, reverse transcriptase; PCR, polymerase chain reaction; kb, kilobase(s); bp, base pair(s).

several transformed human cell lines. We also confirm that the alternative splicing event underlying the formation of the hGRβ message occurs in these tissues. In addition, we show that the unique COOH-terminal end of hGRβ influences several key biochemical properties of this isoform that distinguishes it from hGRα. We demonstrate that hGRβ does not bind glucocorticoids or antiglucocorticoids *in vivo*, resides in the nucleus independent of hormone administration, and in the absence of hGRα is transcriptionally inactive on a glucocorticoid-responsive enhancer. It was recently reported that transfected hGRβ inhibits transfected hGRα-mediated induction of the mouse mammary tumor virus (MMTV) promoter (17). We extend these findings by demonstrating that hGRβ represses the activity of endogenous hGRα and that this hGRβ-mediated repression is a general phenomenon of glucocorticoid-responsive promoters. Thus, the physiological significance of hGRβ may reside in its ability to antagonize the function of hGRα.

EXPERIMENTAL PROCEDURES

Materials—Dexamethasone (DEX) was obtained from Steraloids (Wilton, NH). [^{3}H]DEX (48.2 Ci/mmol) and [^{14}C]chloramphenicol (40–60 mCi/mmol) were obtained from DuPont NEN. RU38486 (RU486) and [^{3}H]RU486 (50.6 Ci/mmol) were kindly provided by Dr. R. Deraedt, Roussel-UCLAF (Romainville, France). [α-^{32}P]UTP (3000 Ci/mmol) was purchased from ICN Radiochemical. The murine leukemia virus reverse transcriptase, *AmpliTaq* DNA polymerase, deoxynucleotide triphosphates, $MgCl_2$, and the RT-PCR buffers were purchased from Perkin-Elmer. Acetyl coenzyme A was obtained from Boehringer Mannheim, and thin layer chromatography sheets were from EM Separations.

Recombinant Plasmids—The hGRα expression vector pCYGR (by Y. Itoh-Lindstrom and J. A. Cidlowski) served as the vector for the expression plasmids pCMVhGRα and pCMVhGRβ utilized in this study. pCYGR was constructed by isolating the 3.0-kb *Kpn*I–*Xho*I cDNA fragment of pRShGRα (3). This fragment (which includes the entire hGRα coding region and the first 384 bp of the hGRα 3′UTR) was then cloned downstream of the human cytomegalovirus major intermediate early gene promoter region in the plasmid pCMV5 (18). The hGRα expression vector pCMVhGRα was constructed by isolating the 3.3-kb *Cla*I–*Bam*HI cDNA fragment from the hGRα clone OB7 (1). This fragment (which contains the distal 940 bp of the hGRα coding region and the 2322 bp hGRα 3′UTR) was then cloned into the *Cla*I–*Bam*HI sites in pCYGR. The hGRβ expression vector pCMVhGRβ was constructed by isolating the 2.3-kb *Cla*I–*Bam*HI cDNA fragment from the hGRβ clone OB10 (1). This fragment (which contains the hGRβ-specific coding sequences as well as the 1430-bp hGRβ 3′UTR) was then cloned into the *Cla*I–*Bam*HI sites in pCYGR. Plasmids pGMCS (19), pGRE2CAT (20), and pBLCAT2 (21) have been previously described.

Cell Culture and Transfections—HeLa S_3 and COS-1 cells were grown as described previously (22, 23). CV-1 cells were grown in Dulbecco's minimum essential medium supplemented with 2 mM glutamine and 10% (v/v) heat-inactivated fetal calf serum. CEM-C7 cells were grown in suspension in RPMI 1640 medium supplemented with 2 mM glutamine and 10% (v/v) heat-inactivated fetal calf serum. All cultures were maintained in a 5% CO_2 humidified atmosphere at 37 °C and were passaged every 3–4 days. HeLa S_3 and COS-1 cells were transfected essentially as described previously (22). Briefly, 4 h before transfection, medium was replaced with fresh Dulbecco's minimum essential medium containing 3% serum. Plasmid DNA was prepared as a calcium phosphate precipitate and incubated with cells for 5 h followed by a 30-s shock with 15% glycerol. Cells were then refed supplemented medium.

Northern Blots—Human adult and fetal multiple tissue Northern blots were purchased from ClonTech (Palo Alto, CA). Membranes were prehybridized and hybridized at 65 °C in 50% formamide, 5 × SSPE, 5 × Denhardt's solution, 2% SDS, 200 μg/ml yeast RNA, 200 μg/ml denatured sheared salmon sperm DNA. ^{32}P-Labeled antisense RNA probes (1×10^6 cpm/ml hybridization fluid) were generated from a T3/T7 promoter-containing vector containing the distal hGRα 3′UTR (537-bp *Pst*I–*Kpn*I fragment from the hGRα clone OB7), the hGRβ coding and proximal 3′UTR (581-bp *Nsi*I–*Sst*I fragment from the hGRβ clone OB10), or the entire hGRα coding region (~3-kb *Kpn*I–*Xho*I fragment from the hGRα expression vector pRShGRα). Following hybridization, blots were washed once at room temperature and four times at 65 °C in 0.1 × SSPE, 0.1% SDS. The blots were then exposed to x-ray film. Membranes were stripped of radioactivity for 30 min in 0.1 × SSPE, 0.1% SDS heated to 100 °C before reprobing.

RT-PCR— Human liver and lung total RNA were kindly provided by Dr. Darryl Zeldin (NIEHS). Human heart, brain, and skeletal muscle total RNA was purchased from ClonTech. Total RNA from HeLa S_3 and CEM-C7 cells was isolated using TRIzol Reagent (Life Technologies, Inc.) according to the manufacturer's instructions. cDNA was prepared in a buffer containing 10 mM Tris-HCl, pH 8.3, 50 mM KCl, 5 mM $MgCl_2$, 1 mM each dGTP, dATP, dTTP, and dCTP, 20 units RNase inhibitor, 50 units murine leukemia virus reverse transcriptase, 2.5 μM random hexamers, 1.0 μg of sample RNA, in a final volume of 20 μl. This mixture was incubated for 10 min at RT, 15 min at 42 °C, and 5 min at 99 °C and then used for amplification of specific cDNAs by PCR. The buffer for PCR contained 10 mM Tris-HCl, pH 8.3, 50 mM KCl, 2 mM $MgCl_2$, 2.5 units *AmpliTaq* DNA polymerase, 0.2 μM upstream and downstream primers, in a final volume of 100 μl. After an initial incubation for 1 min at 95 °C, samples were subjected to 45 cycles of 30 s at 95 °C, 30 s at 62 °C, and 30 s at 72 °C. This was followed by a final extension step at 72 °C for 10 min. The primers used for the amplification of the 7.0-kb hGR message were as follows: 5′-GCATTCATACAGGCAGCGAT-3′ (upstream) and 5′-CCACGTATCCTAAAAGGGCAC-3′ (downstream) corresponding to nucleotides 4221–4240 and 2503–2523 of the hGRα and hGRβ cDNAs, respectively (1). The primers used for the amplification of the hGRα message were as follows: 5′-CCTAAGGACGGTCTGAAGAGC-3′ (upstream) and 5′-GCCAAGTCTTGGCCCTCTAT-3′ (downstream), corresponding to nucleotides 2158–2178 and 2616–2635 of the hGRα cDNA (1). The primers used for the amplification of the hGRβ message were as follows: 5′-CCTAAGGACGGTCTGAAGAGC-3′ (upstream) and 5′-CCACGTATCCTAAAAGGGCAC-3′ (downstream), corresponding to nucleotides 2158–2178 and 2503–2523 of the hGRβ cDNA (1). Amplified DNA fragments were electrophoretically fractionated on 1.75% agarose gels. Restriction enzyme analysis of the RT-PCR products amplified by the hGRα- and hGRβ-specific primers confirmed that these fragments contained the appropriate hGRα and hGRβ cDNA sequences. Restriction enzymes employed included *Nsi*I (specific to exon 8), *Ssp*I (specific to exon 9α), and *Hae*II (specific to exon 9β).

Quantitative RT-PCR—Human RNA (0.5 μg) was reverse transcribed, and the resulting cDNA was amplified as described above. 5 μl of the PCR reaction was removed at 2-cycle intervals and electrophoresed on 1.75% agarose gels stained with ethidium bromide. The intensity of the ethidium bromide fluorescence was measured densitometrically and plotted as a function of cycle number to generate amplification curves for the hGRα and hGRβ PCR fragments. Regression equations of the form $y = a \times b^n$, where y is the intensity and n is the number of cycles, were fitted to the data in the linear portion of the semi-logarithmic graphs. The amplification efficiencies (E) for the hGRα and hGRβ fragments, while nearly identical within tissues, varied slightly across tissues: $E\alpha = 0.71$ and $E\beta = 0.71$ for CEM-C7 cells but $E\alpha = 0.82$ and $E\beta = 0.81$ for human lung. Amplification curves were also generated (and regression equations fitted) for external standards containing linearized pCMVhGRβ and pCMVhGRα at ratios of 1:1000, 10:1000, 100:1000, and 1000:1000, respectively. A standard curve was generated by plotting the difference in the number of cycles required to amplify (during the exponential phase of each reaction) an identical amount of the hGRα and hGRβ PCR products (3000 densitometric units) as a function of the pCMVhGRβ/pCMVhGRα ratio. Similarly, the difference in the number of cycles required to amplify (during the exponential phase of each reaction) the same amount of hGRα and hGRβ PCR products (3000 densitometric units) for each human sample was calculated. Using the standard curve regression equation, the approximate hGRβ/hGRα cDNA (and hence mRNA) ratio was determined for each human tissue and cell line.

Sucrose Density Gradients and Western Blots—Subconfluent COS-1 cells (4×10^6) were transfected by the calcium phosphate method as described above with equimolar amounts of pCMVhGRα (40 μg), pCMVhGRβ (36.4 μg), or pCMV5 (20.4 μg). Each transfection was standardized to 40 μg of DNA using pBR322. Cells were harvested 48 h post-transfection, resuspended in unsupplemented Dulbecco's minimum essential medium containing 100 nM [^{3}H]DEX or 20 nM [^{3}H]RU486, and incubated for 2 h on ice with gentle agitation. Whole cell extracts were prepared and processed on sucrose density gradients essentially as described by Tully and Cidlowski (24). To verify equivalent expression of the hGRα and hGRβ proteins, an aliquot of each extract was analyzed by Western blotting. Proteins (125 μg) were resolved by electrophoresis through 7.5% polyacrylamide gels and electrophoretically transferred to nitrocellulose. After incubating the membrane with epitope-purified polyclonal anti-hGR antiserum #57 (25) at a dilution of 1:2000, immunoreactivity was visualized using enhanced chemiluminescence accord-

ing to the manufacturer's instructions (ECL, Amersham Corp.).

Immunohistochemistry—Subconfluent COS-1 cells (2×10^5) were transfected with equimolar amounts of pCMVhGRα (20 μg) or pCMVhGRβ (18.2 μg) by the calcium phosphate method as described above or by the DEAE method of Sompayrac and Danna (26) as modified by Gorman (27). Each transfection was standardized to 20 μg of DNA using pBR322. Following transfection, the cells were incubated for 24 h in Dulbecco's minimum essential medium supplemented with 10% dextran-coated charcoal-treated serum before plating in two-chamber glass slides. After an additional 24-h incubation, transfected cells were treated for 2 h with DEX (100 nM) or control vehicle and processed for immunohistochemical staining as described previously (25). Immunoreactivity was visualized by staining with avidin-biotin-peroxidase or Texas red fluorescent dye.

CAT Activity—Subconfluent COS-1, CV-1, and HeLa S_3 cells were transfected as indicated in the appropriate figure legends by the calcium phosphate method described above. 16 h post-transfection, medium was removed and replaced with control medium or medium containing DEX or RU486. Cells were harvested 24 h later and CAT assays were performed as described previously (22).

RESULTS

Northern Blot Analysis of the hGRβ Message in Human Tissues and Cell Lines—Northern blot analysis of RNA isolated from various human cell lines routinely shows multiple hGR mRNA transcripts approximately 7.0 and 5.0 kb in size (1, 28–33). These transcripts are thought to arise from the use of alternative polyadenylation signals within the 3′UTR of exon 9α and are presumed to encode the hGRα isoform. Because early studies utilized probes that recognized a region common to the hGRα and hGRβ messages, one or more of these transcripts might actually be the hGRβ splice variant. In order to discriminate between hGRα and hGRβ messages and to assess the relative amounts of these transcripts in a given tissue, we sequentially hybridized poly(A)$^+$ RNA isolated from various human adult and fetal tissues with hGRβ- and hGRα-specific cRNA riboprobes. The hGRβ riboprobe was designed to recognize a 578-nucleotide segment spanning the coding and proximal 3′ noncoding regions of exon 9β. The hGRα riboprobe was designed to recognize a 534-nucleotide segment in the distal 3′UTR of exon 9α.

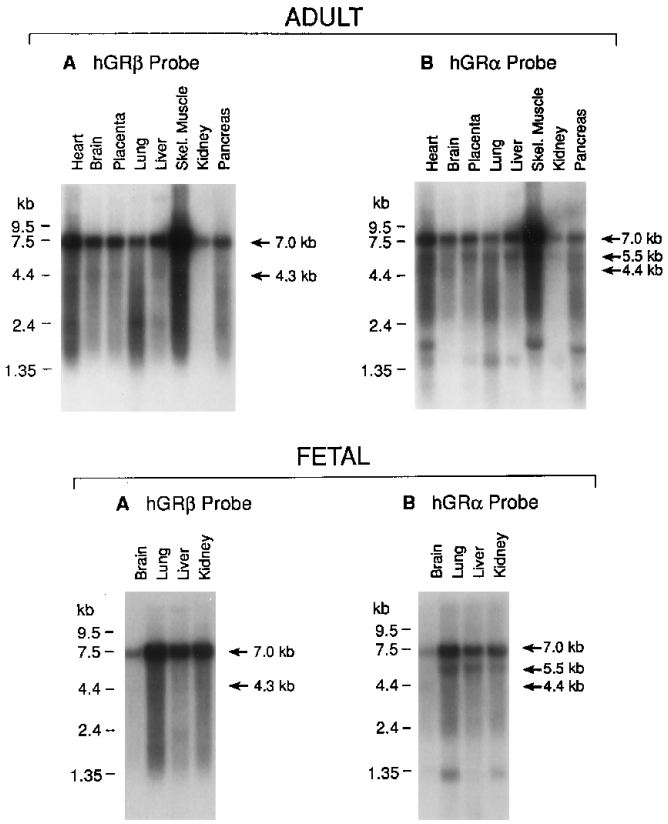

FIG. 1. **Northern blot analysis of hGR messages in human adult (*upper panel*) and fetal (*lower panel*) tissues.** Human adult and fetal multiple tissue Northern blots containing 2.0 μg of poly(A)$^+$ RNA were hybridized with the hGRβ-specific riboprobe (*A*, *both panels*). The blots were then stripped and rehybridized with the hGRα-specific riboprobe (*B*, *both panels*). RNA size markers are indicated along the *left margin*, and the approximate sizes of the hybridization signals are indicated along the *right margin*.

As shown in Fig. 1*A* (*upper* and *lower panels*), the hGRβ probe hybridizes with an abundant message in all tissues migrating slightly below the 7.5-kb RNA marker. Additionally, a faint band slightly below the 4.4-kb RNA marker is observed in the adult heart, brain, placenta, lung, liver, skeletal muscle, and pancreas RNA samples and in the fetal brain, lung, and liver RNA samples. The length of the hGRβ cDNA predicts the hGRβ message to be at least 4.1 kb in size, thus the lower hybridization signal (approximately 4.3 kb in size) may correspond to the hGRβ mRNA transcript. In contrast to the lower hybridization signal, the abundant message approximately 7.0 kb in size cross-reacts with the hGRα riboprobe (Fig. 1*B*, *upper* and *lower panels*). The hGRα riboprobe also hybridizes with a message approximately 5.5 kb in size in many tissues and with a less abundant 4.4 kb message in several tissues, and these two transcripts do not appear to cross-react with the hGRβ probe (Fig. 1*B*, *upper* and *lower panels*). Finally, the hGR mRNA transcripts approximately 7.0, 5.5, and 4.3 kb in size are all recognized by a probe made to the common coding region of the hGRα and hGRβ cDNAs (data not shown). Similar hybridization patterns are also observed on Northern blots of RNA isolated from HeLa S_3 cells (a human cervical carcinoma cell line) and CEM-C7 cells (a human lymphoid cell line) (data not shown).

Characterization of the 7.0-kb hGR Message—Because the 7.0-kb hGR message is recognized by both the hGRα and hGRβ riboprobes, it must contain information from both the 9α and 9β exons. These exons, therefore, do not appear to be mutually exclusive as previously reported (2). This observation made it important to determine whether the 7.0-kb message encodes the hGRα or hGRβ isoform. Various data suggested that it would encode hGRα. Exon 9α precedes exon 9β in the linear organization of the hGR gene (2). If this order is maintained in the mature message, exon 9α would form the distal coding and proximal 3′ noncoding regions, and exon 9β would comprise the distal 3′ noncoding region. A hGR message with this arrangement at its 3′ end would be expected to encode the hGRα protein. Sequence conservation between hGR exons 9α and 9β (as well as the 155-bp intron separating these two exons) and the distal coding and 3′ noncoding regions of the 6.5-kb rat GR message (Fig. 2*A*) further suggested that the 7.0-kb hGR mRNA transcript contains (moving 5′ to 3′) exon 9α, intron J, and exon 9β sequences at its distal 3′ end. If all 10 exons and intron J of the hGR gene are represented in a mature hGR message, this message would be approximately 6.8 kb in size, consistent with the size of the hybridization signal observed on our Northern blots.

To test whether the 3′ end of the 7.0-kb hGR message is organized in this fashion, we performed RT-PCR using a sense 5′ primer specific to the distal 3′UTR of exon 9α and an antisense 3′ primer specific to the proximal 3′UTR of exon 9β. If the 3′ end of the 7.0-kb hGR message consists of sequences from exon 9α, intron J, and exon 9β, these primers will amplify a 933-bp PCR product. When total RNA extracted from HeLa S_3 cells is used for RT-PCR, a PCR product of this size is generated (Fig. 2*B*, *lane 2*). The PCR fragment is not produced when the reverse transcriptase is omitted from the reaction, demonstrating that contaminating DNA is not present (Fig. 2*B, lane 1*). In

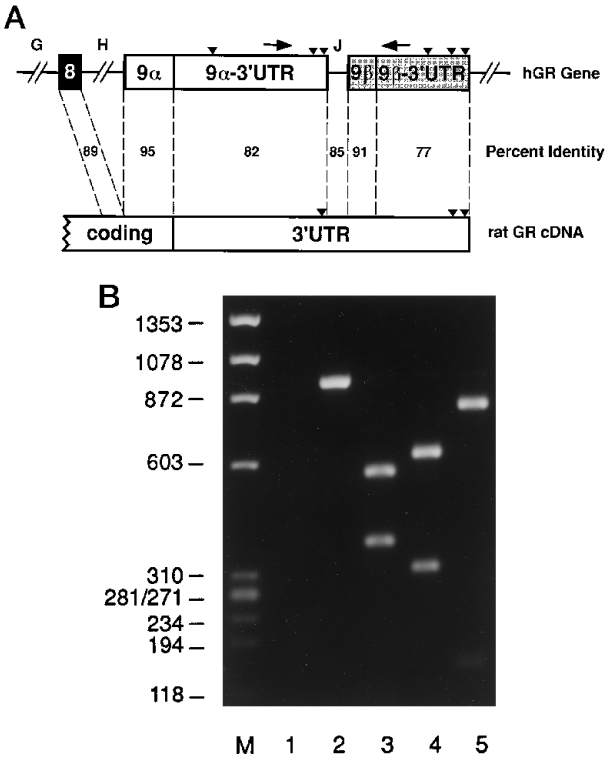

FIG. 2. **Comparison of hGR exons 9α and 9β and intron J with the rat GR cDNA (*A*) and RT-PCR analysis of the 7.0 kb hGR message (*B*).** *A*, using the sequence comparison program BestFit (Sequence Analysis Software Package, Genetics Computer Group, University of Wisconsin Biotechnology Center) (34), the hGRα cDNA sequences 2156–2313 (exon 8), 2314–2466 (exon 9α coding), and 2467–4788 (exon 9α 3′UTR) (1); intron J sequences 1–155 (2); and the hGRβ cDNA sequences 2314–2361 (exon 9β coding) and 2362–3791 (exon 9β 3′UTR) (1) were aligned with the rat GR cDNA sequences 1–6322 (35). The regions of greatest similarity and the percentage of identity between the two aligned sequences are indicated. *Triangles* identify consensus polyadenylation signals, and *arrows* indicate the location of PCR primers utilized in *B*. *B*, total RNA (1.0 μg) from HeLa S_3 cells was reverse transcribed using random hexamers, and first strand cDNA was subsequently amplified with the addition of an upstream primer specific to the distal 3′UTR of exon 9α and a downstream primer specific to the proximal 3′UTR of exon 9β. The resulting RT-PCR products were then analyzed by agarose gel electrophoresis. The reverse transcriptase was omitted in *lane 1* but included in *lane 2*. In *lanes 3–5*, the PCR product was digested with restriction enzymes that cut specifically in exon 9α (*Acc*65I), intron J (*Hpa*II), or exon 9β (*Hae*II). Sizes (in bp) of DNA markers (*M*) are indicated in the *left margin*.

addition, restriction enzymes that cleave sites specific to exon 9α, intron J, and exon 9β were used to confirm the sequence of the 933-bp PCR fragment (Fig. 2*B*, *lanes 3–5*). Therefore, exon 9α makes up the distal coding and proximal 3′ noncoding regions of the 7.0-kb hGR message and both intron J and exon 9β form the distal 3′ noncoding region of the 7.0-kb hGR message. This message would be expected to encode the hGRα isoform.

These RT-PCR results also demonstrate that sequences previously identified as intron J (2) are actually exonic sequences separating the 9α and 9β exonic sequences. In agreement with this finding, an oligonucleotide probe specific to intron J hybridizes on Northern blots with the 7.0-kb hGRα message (data not shown). Therefore, we propose that the hGR sequences formerly identified as exon 9α, intron J, and exon 9β comprise one large terminal exon (exon 9) approximately 4.1-kb in size and that the hGR gene is organized into nine exons rather than the previously reported ten (2).

RT-PCR Analysis of the hGRβ Message in Human Tissues and Cell Lines—The hGRβ-specific riboprobe also hybridizes with a faint message approximately 4.3 kb in size on the Northern blots shown in Fig. 1. The size of this message suggests that it might be the hGRβ mRNA transcript. However, because the 7.0-kb hGRα message contains the 9β sequences at its 3′ end, the 4.3-kb signal might instead be a degradation product of the 7.0-kb hGRα message. Alternatively, the 4.3-kb signal might represent nonspecific hybridization of the hGRβ probe with 28 S rRNA. Recently, it was reported using RT-PCR that the alternative splicing event underlying the formation of the hGRβ mRNA transcript occurs in many different human tissues (17). However, these experiments employed a very large number of PCR cycles, and these workers apparently did not control for potential amplification of contaminating DNA. Therefore, to confirm that the hGRβ message is expressed, we performed RT-PCR on RNA isolated from various human tissues and cell lines using primers that hybridize on either side of the alternatively spliced region of the 4.3-kb hGRβ message.

A sense 5′ primer specific to exon 8 and an antisense 3′ primer specific to the 9β sequences were utilized in the PCR reaction. If the alternative splicing event underlying the formation of the 4.3-kb hGRβ message occurs (in which the end of exon 8 is linked to the 9β sequences located in the distal portion of exon 9) the hGRβ-specific primers will produce a PCR product 366-bp in length. If these primers hybridize with the 7.0-kb hGRα message (which also contains the 9β sequences at its far 3′ end), they will generate a PCR product approximately 3000 bp in length. Conditions of our PCR amplification reaction did not favor production of this large PCR fragment, and it was never observed. For parallel analysis of the hGRα mRNA transcripts, an antisense 3′ primer specific to the 9α sequences was used in combination with the same sense 5′ primer. If the default splicing event underlying the formation of the hGRα messages occurs (in which the end of exon 8 is linked to the 9α sequences at the beginning of exon 9) these hGRα-specific primers will produce a PCR product 477 bp in length.

When total RNA extracted from human heart, brain, lung, liver, and skeletal muscle is used for RT-PCR, a 366-bp PCR product is generated by the hGRβ-specific primers, suggesting that the hGRβ message is present in these human tissues (Fig. 3*A*). In addition, the hGRα-specific primers amplify the expected 477-bp PCR product in each tissue (Fig. 3*B*). When the reverse transcriptase is omitted from the RT-PCR reaction, the expected PCR fragments are not produced, indicating that only cDNA produced by the RT step is serving as template for the correctly sized PCR product. RT-PCR analysis was also performed on RNA isolated from HeLa S_3 and CEM-C7 cells (Fig. 3, *A* and *B*). Again, a 366-bp PCR fragment is produced by the hGRβ-specific primers, suggesting that the hGRβ message is present in these transformed human cell lines. Consistent with our Northern blot data, the hGRβ message appears to have a widespread tissue distribution.

Together, the Northern blot and RT-PCR analyses indicate that the hGR mRNA heterogeneity observed in human tissues and cell lines includes both hGRα and hGRβ messages. The more abundant transcripts are approximately 7.0 and 5.5 kb in size and are expected to encode the hGRα isoform. Consensus polyadenylation signals are located at the end of the 9α sequences in exon 9, and use of these signals would generate a hGRα message approximately 1.6 kb shorter than the full-length 7.0-kb hGRα message. These consensus signals are functional because they terminate transcription of the hGRα cDNA cloned into an expression vector lacking other polyadenylation signals (data not shown). Therefore, the 5.5-kb hGRα message appears to originate from alternative polyadenylation at these consensus sites. The less abundant hGR message recognized by the hGRβ-specific probe and approxi-

mately 4.3 kb in size is expected to encode the hGRβ isoform. This mRNA transcript results from alternative splicing in which a 3′ acceptor site preceding the 9β sequences in exon 9 is utilized by the splicing machinery rather than the normal 3′ acceptor site preceding the 9α sequences in exon 9. The model shown in Fig. 4 summarizes the predicted structure at the 3′ end of the hGR gene, primary transcript, and mature hGRα and hGRβ mRNAs; the processing events underlying the formation of these mature messages; and the predicted translation products of these transcripts.

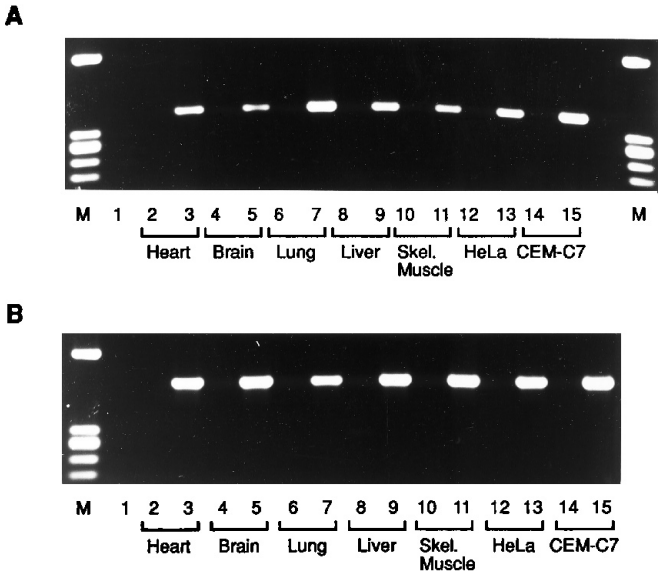

FIG. 3. **RT-PCR analysis of RNA isolated from human tissues and cell lines using hGRβ- and hGRα-specific primers.** Total RNA (0.5 μg) isolated from various human adult tissues (heart, brain, lung, liver, and skeletal muscle) and cell lines (HeLa S_3 and CEM-C7 cells) was reverse transcribed using random hexamers. The resulting cDNA was amplified using either hGRβ-specific (*A*) or hGRα-specific (*B*) primers. For each set of primers, the reverse transcriptase was omitted in *lanes 2*, *4*, *6*, *8*, *10*, *12*, and *14* but included in *lanes 3*, *5*, *7*, *9*, *11*, *13*, and *15*. No RNA was added in *lane 1*. The RT-PCR products were analyzed by agarose gel electrophoresis. The sizes (in bp) of the DNA markers (*M*) are 603, 310, 281/271, 234, and 194).

Based on the intensity of the Northern blot signals, the two hGRα messages (7.0 and 5.5 kb) are much more abundant than the 4.3-kb hGRβ message (see Fig. 1). To more accurately assess the relative levels of the hGRα and hGRβ mRNA transcripts, we performed quantitative RT-PCR on RNA isolated from adult lung, adult liver, HeLa S_3 cells, and CEM-C7 cells. Reaction cycle intensity curves for the 477-bp hGRα and 366-bp hGRβ PCR products are shown for each tissue and cell line in Fig. 5*A*. For estimation of the hGRβ/hGRα mRNA ratio, regression equations were fitted to the linear portion of each amplification curve, and the difference in the number of cycles required to amplify an equal amount of hGRα and hGRβ PCR product was calculated. Similarly, the difference in cycle number required to amplify an equal amount of hGRα and hGRβ PCR product was determined for a series of external standards containing known hGRβ/hGRα cDNA ratios. Using the standard curve shown in Fig. 5*B*, the hGRβ/hGRα cDNA (and hence mRNA) ratio for each human sample was calculated and is as follows: 0.34% for lung, 0.21% for liver, 0.21% for HeLa S_3 cells, and 0.22% for CEM-C7 cells. Although these values reflect a large difference in expression levels, one should bear in mind that the amount of the 477-bp hGRα fragment is derived from two hGRα messages (7.0 and 5.5 kb), whereas the amount of 366-bp hGRβ fragment comes only from the 4.3-kb hGRβ message. In addition, our approach assumes that the efficiency of the RT reaction is the same for both the hGRα and hGRβ mRNA transcripts. This may not be the case.

Ligand Binding Analysis of hGRβ—Operating under the

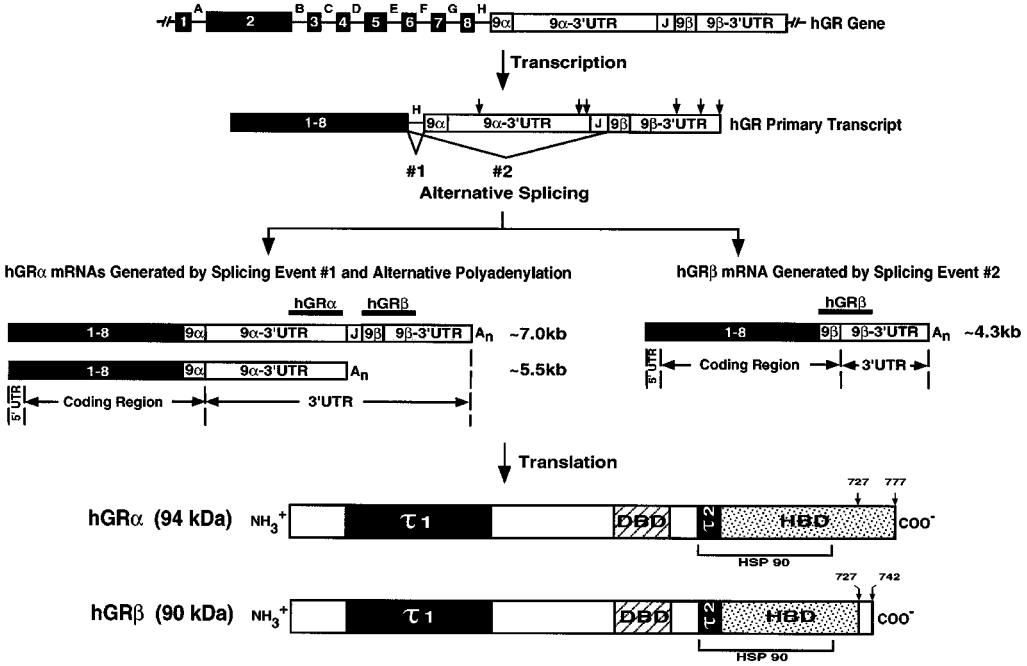

FIG. 4. **Predicted structure of the hGR gene and gene products.** hGR sequences formerly identified as exon 9α, intron J, and exon 9β comprise one large exon (exon 9). Alternative processing of exon 9 generates multiple hGR messages. Specifically, splicing event #1 (default splicing pathway) in which the end of exon 8 is linked to beginning of exon 9 is predicted to generate the 7.0- and 5.5-kb hGRα messages, which differ in size due to the use of alternative polyadenylation signals. Splicing event #2 (alternative splicing pathway) in which the end of exon 8 is linked to the beginning of the 9β sequences is predicted to generate the 4.3-kb hGRβ message. Translation of the messages produces the hGRα and hGRβ isoforms, which are identical through amino acid 727 but then diverge. The functional domains and the putative site of hsp90 interaction are indicated for each isoform. Exons and introns (not to scale) are designated by *boxes* and *lines*, respectively. The *arrows* along the primary transcript identify the location of consensus polyadenylation signals. Splicing of introns *A–G* is not shown. The hGRα- and hGRβ-specific cRNA probes used in this study are indicated by *solid lines*.

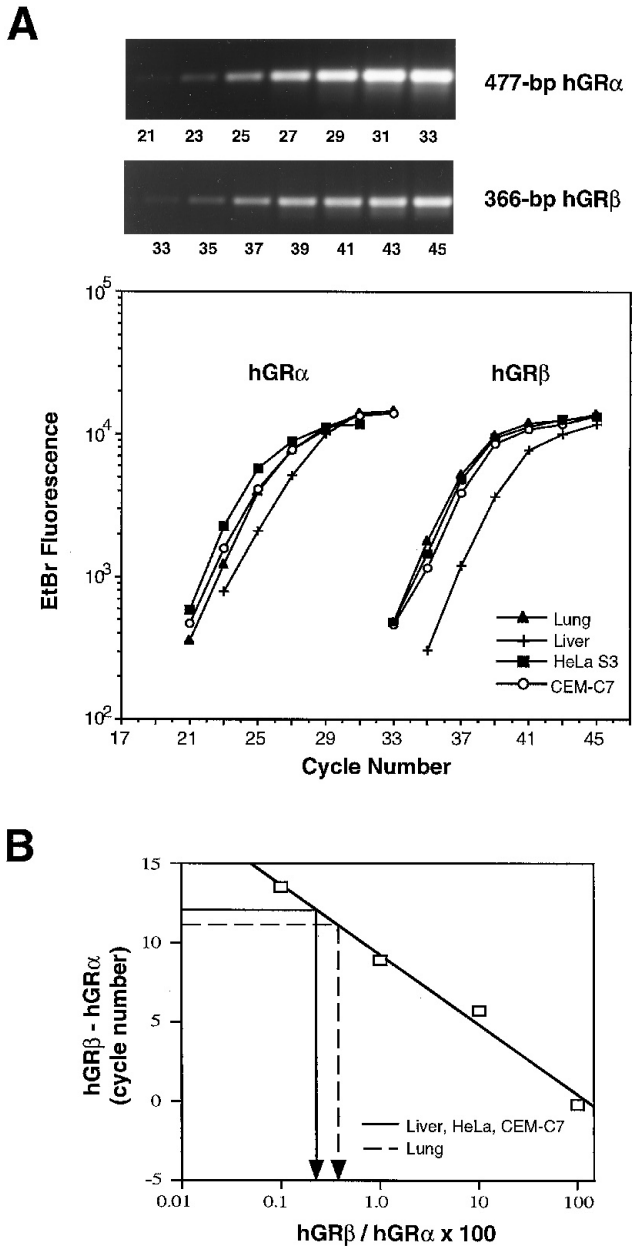

FIG. 5. **Quantitative RT-PCR analysis of hGR*α* and hGR*β* messages.** *A*, human RNA (0.5 μg) was reverse transcribed, and the resulting cDNA amplified using hGRα- or hGRβ-specific primers. Aliquots of the PCR reaction were removed at 2-cycle intervals and electrophoresed on agarose gels stained with ethidium bromide. Representative gels showing amplification of the 477-bp hGRα and 366-bp hGRβ fragments are from human lung (*upper panel*). By plotting ethidium bromide fluorescence as a function of cycle number, hGRα and hGRβ amplification curves were generated for adult lung, adult liver, HeLa S_3 cells, and CEM-C7 cells (*lower panel*). *B*, standard curve showing the relationship between a known hGRβ/hGRα cDNA ratio and the additional number of cycles required by the hGRβ primers to amplify as much PCR product as the hGRα primers. "Cycle number difference" calculations are from the exponential phase of each PCR reaction and are described under "Experimental Procedures." For each human tissue and cell line, the standard curve regression equation $y = -4.427\text{LOG}(x) + 0.297$ ($r = 0.994$) was used to determine the hGRβ/hGRα cDNA (and hence mRNA) ratio.

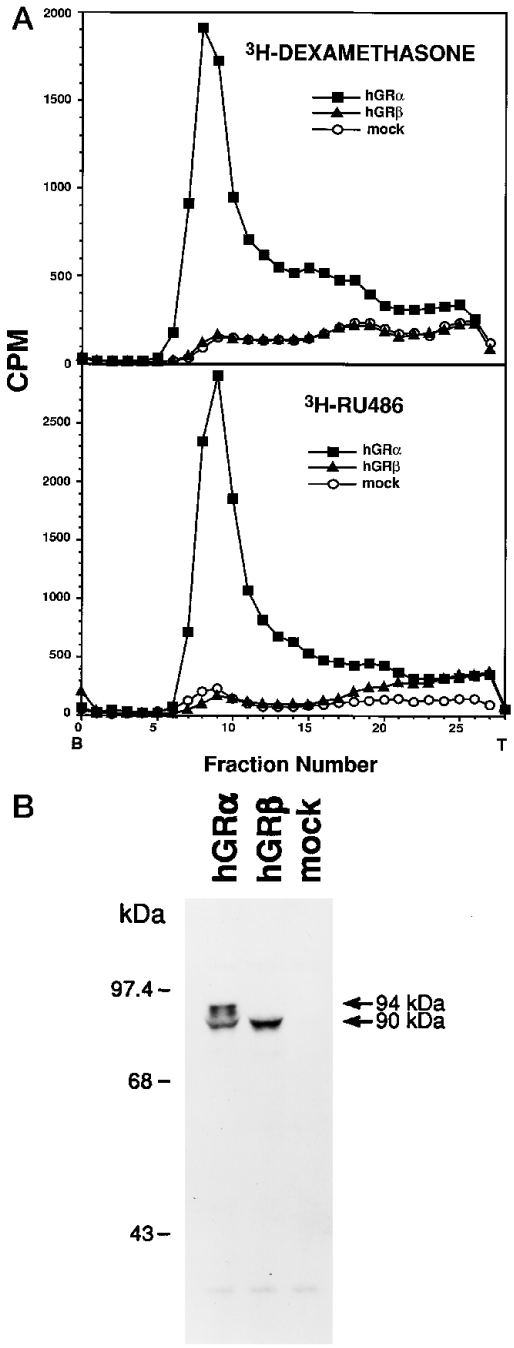

FIG. 6. ***In vivo* ligand binding analysis of hGR*β* expressed in transfected COS-1 cells.** *A*, COS-1 cells were transfected with equimolar amounts of pCMVhGR*α*, pCMVhGR*β*, or pCMV5 (mock) as described under "Experimental Procedures" and incubated with 100 nM [^{3}H]dexamethasone (*upper panel*) or 50 nM [^{3}H]RU486 (*lower panel*) for 2 h on ice. Whole cell extracts were prepared and loaded on 5–20% sucrose gradients. Following centrifugation, the gradients were fractionated, and radioactivity was determined. *B* refers to the bottom of the gradient, and *T* refers to the top. *B*, a portion of each whole cell extract was analyzed by Western blotting using the anti-hGR antibody #57 (25) that recognizes an epitope common to the 94-kDa hGRα and 90-kDa hGRβ proteins. Molecular mass standards are indicated in the *left margin*.

assumption that the endogenous hGRβ message is translated into the endogenous hGRβ protein, we began investigating the biochemical properties of hGRβ when overexpressed in transfected COS-1 cells. COS-1 cells contain undetectable levels of endogenous GR (3) and therefore provide a model system for studying the biochemical properties of hGRβ in the absence of hGRα. The carboxyl-terminal 50 amino acids of hGRα have been replaced in hGRβ with 15 unique amino acids. To investigate the effect this has on the ability of hGRβ to bind hormone or antihormone, we transfected COS-1 cells with a hGRα expression vector (pCMVhGRα), a hGRβ expression vector (pCMVhGRβ), or the expression vector backbone (pCMV5). The

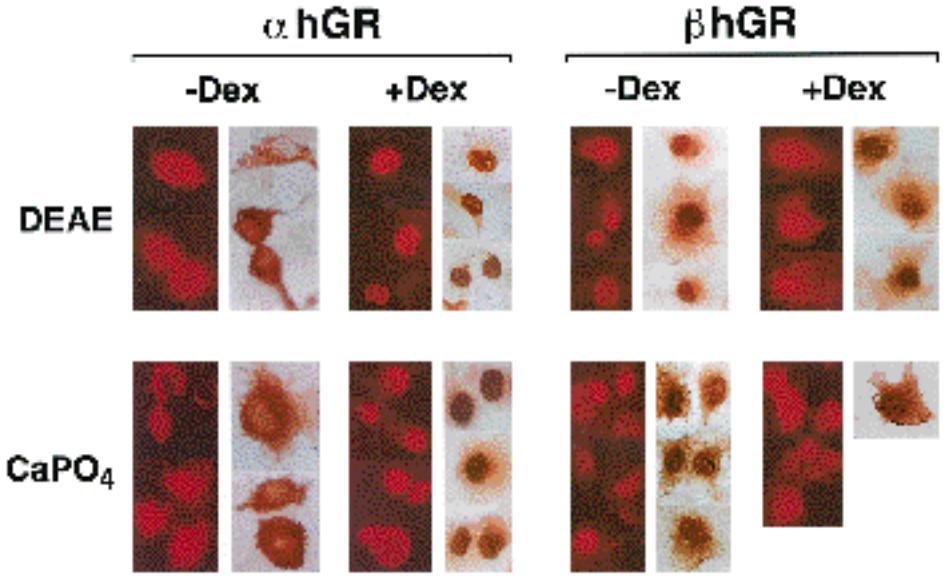

FIG. 7. **Subcellular distribution of hGRβ expressed in transfected COS-1 cells.** COS-1 cells were transfected with equimolar amounts of pCMVhGRα (*left panel*) or pCMVhGRβ (*right panel*) using either the DEAE or calcium phosphate ($CaPO_4$) transfection methods as described under "Experimental Procedures." 36 h post-transfection, cells were treated for 2 h with vehicle (−*Dex*) or with 100 nM DEX (+*Dex*). Immunohistochemistry was then performed using the anti-hGR antibody #57 (25), and immunoreactivity was visualized by staining with Texas red fluorescent dye (*left side*, each subpanel) or avidin-biotin-peroxidase (*right side*, each subpanel).

cells were incubated with radiolabeled DEX, a synthetic glucocorticoid agonist, or radiolabeled RU486, a synthetic glucocorticoid antagonist. [^{3}H]Steroid-receptor complexes formed *in vivo* were then analyzed by sucrose density gradients. Showing the standard sedimentation profile for the 8 S unactivated GR (24), hGRα binds both [^{3}H]DEX and [^{3}H]RU486 (Fig. 6*A*). In contrast, hGRβ does not appear to bind either of these ligands, because the sedimentation profiles for the pCMVhGRβ- and pCMV5-transfected cells are superimposable. Western blot analysis of the extracts analyzed for hormone binding demonstrates that both the 94-kDa hGRα and 90-kDa hGRβ isoforms were synthesized at similar levels (Fig. 6*B*). Therefore, lack of steroid binding by hGRβ is not due to insufficient expression of the hGRβ protein. Interestingly, the hGRα expression vector does not contain the hGRβ-specific sequences, yet a 90-kDa protein is observed in the pCMVhGRα-transfected cells (Fig. 6*B*). This protein, which cannot be hGRβ, appears to be a degradation product or post-translational modification of the 94-kDa hGRα isoform.

Subcellular Distribution of hGRβ—Numerous studies have shown that hGRα resides in the cytoplasm of cells in the absence of hormone and translocates to the nucleus in a hormone-dependent manner (11). To determine where hGRβ is localized within a given cell, COS-1 cells were transiently transfected with the hGRα or hGRβ expression vectors. The plasmids were delivered into the cells using either the DEAE-dextran or calcium phosphate transfection method to rule out potential artifacts due to the transfection procedure. After treating the cells for 2 h with or without DEX, immunohistochemistry was performed, and immunoreactivity was visualized by staining with Texas red fluorescent dye or avidin-biotin-peroxidase. In the absence of hormone hGRα is found in the cytoplasm of the transfected cells, but following hormone administration it translocates and becomes predominantly nuclear (Fig. 7, *left panel*). In contrast, the hGRβ protein resides primarily in the nucleus of the transfected cells independent of hormone treatment (Fig. 7, *right panel*). These findings were consistent regardless of the transfection method or immunohistochemical staining procedure employed.

Transcriptional Activity of hGRβ in the Absence of hGRα—hGRβ does not appear to bind hormone or antihormone, but it resides primarily in the nucleus of transfected COS-1 cells (and CV-1 cells)[2] and has been reported to bind a consensus GRE *in vitro* (17). Therefore, we investigated the ability of hGRβ to activate or repress the glucocorticoid-responsive MMTV enhancer in the presence or the absence of steroid. For these experiments, COS-1 cells were cotransfected with an MMTV-CAT reporter plasmid (pGMCS) and either pCMV5, pCMVhGRα, or pCMVhGRβ. In response to DEX, hGRα induces a 4-fold increase in CAT expression over that observed in the vehicle-treated cells, whereas RU486 alone has little or no effect (Fig. 8*A*, *lanes 4–6*). In contrast, CAT expression is unchanged in the hGRβ-containing cells treated with steroid, which is consistent with the inability of hGRβ to bind these ligands (Fig. 8*A*, *lanes 7–9*). Moreover, hGRβ does not appear to be constitutively active as an enhancer or repressor because levels of CAT activity in the vehicle-treated cells are similar whether they contain the CMV-vector backbone or pCMVhGRβ (Fig. 8*A*, compare *lanes 1 and 7*).

The hGRα-mediated induction of CAT activity in transfected COS-1 cells was only 4-fold. In cell lines where hGRα inductions are much greater, hGRβ might display partial transcriptional activity. Therefore, we investigated the transcriptional activity of hGRβ on the MMTV enhancer in receptor negative CV-1 cells. In response to DEX, hGRα induces a 74-fold increase in CAT expression (Fig. 8*B*, *lanes 4 and 5*). Interestingly, hGRα induces a 29-fold increase in CAT expression in response to RU486 (Fig. 8*B*, *lanes 4 and 6*). This partial agonist activity of RU486 has been reported previously and appears to be cell type-specific (37). Consistent with our findings in COS-1 cells, CAT expression is unchanged in CV-1 cells transfected with hGRβ and treated with steroid (Fig. 8*B*, *lanes 7–9*). In addition, hGRβ does not appear to be constitutively active (Fig. 8*B*, compare *lanes 1 and 7*). Thus, we conclude that in the absence of hGRα, hGRβ is transcriptionally inactive on the glucocorticoid-responsive MMTV enhancer.

Transcriptional Activity of hGRβ in the Presence of hGRα—In the absence of hGRα, hGRβ is unable to directly enhance or repress transcription of the MMTV-CAT reporter plasmid. To determine if hGRβ influences gene expression indirectly by modulating the transactivation capacity of hGRα, HeLa S_3 cells (which contain approximately 20,000 hGRα receptors per cell) were cotransfected with pGMCS and various

[2] R. H. Oakley and J. A. Cidlowski, unpublished observations.

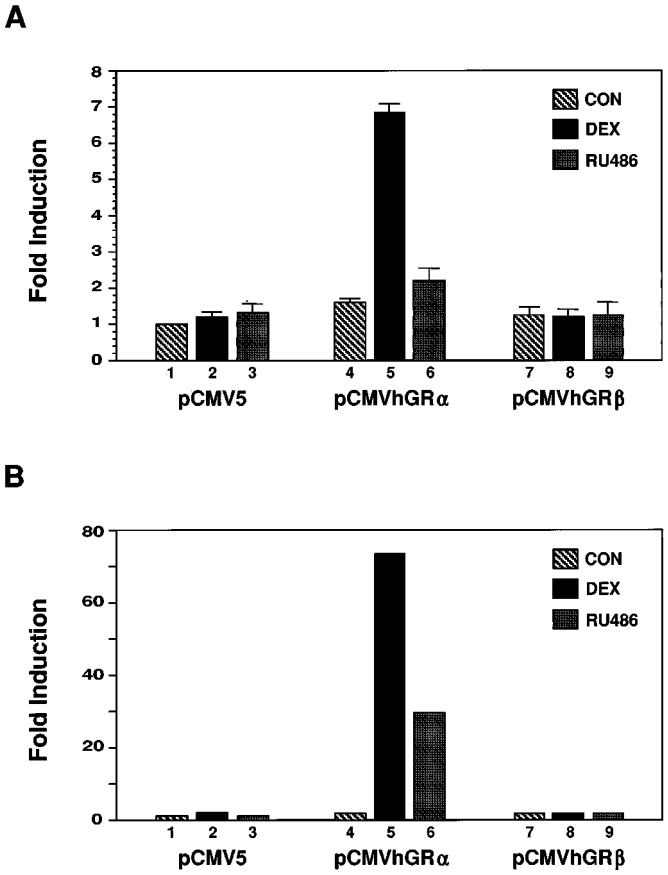

FIG. 8. **Transcriptional activity of hGRβ in the absence of hGRα.** COS-1 (*A*) or CV-1 (*B*) cells were cotransfected with pGMCS (5.0 μg) and equimolar amounts of pCMV5 (2.8 μg), pCMVhGRα (5.5 μg), or pCMVhGRβ (5.0 μg). Each transfection was standardized to 10.5 μg of DNA using pBR322. 16 h post-transfection, medium containing vehicle (*CON*), 100 nM DEX, or 1 μM RU486 was added to the cells, which were then incubated an additional 24 h. Cells were then harvested, and CAT activity was determined. The data are plotted as fold change from basal activation (pCMV5, *CON*). *A* shows the average of three independent experiments, and *B* is representative of three independent experiments.

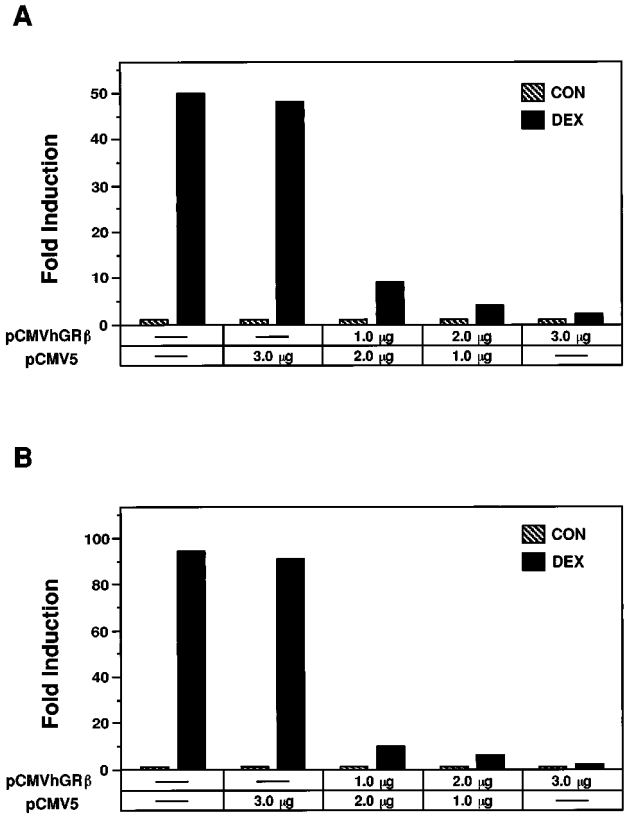

FIG. 9. **Transcriptional activity of hGRβ in the presence of hGRα.** HeLa S_3 cells were cotransfected with 5.0 μg of pGMCS (*A*) or pGRE2CAT (*B*) and various amounts of pCMV5 and pCMVhGRβ as indicated. 16 h post-transfection, medium containing vehicle (*CON*) or 100 nM DEX was added to the cells, which were then incubated an additional 24 h. Cells were then harvested, and CAT activity was determined. The data are plotted as fold change from basal activation and are representative of three independent experiments.

amounts of pCMVhGRβ (Fig. 9*A*). When pGMCS alone is transfected into the cells, DEX treatment results in a 50-fold induction of CAT activity. However, as increasing amounts of pCMVhGRβ are transfected into the cells, the glucocorticoid-induced, hGRα-mediated activation of the MMTV enhancer is repressed in a dose-dependent manner. We observe a 78 and 96% inhibition of CAT expression when 1.0 and 3.0 μg, respectively, of pCMVhGRβ is used in the transfection mixture. Transfection of a 2-fold molar excess of the CMV-vector backbone (pCMV5) has no effect on hGRα-mediated induction of CAT expression, indicating that hGRβ is responsible for the repression.

We next evaluated whether the dominant negative activity of hGRβ on hGRα-mediated transcription is restricted to the MMTV promoter or is a general property of glucocorticoid-responsive promoters. The pGRE2CAT reporter plasmid contains two copies of the GRE consensus sequence derived from the tyrosine aminotransferase gene and a TATA box element upstream of the CAT gene (20). In contrast to MMTV, this "minimal promoter" does not contain binding sites for other ancillary transcription factors. When HeLa S_3 cells are cotransfected with pGRE2CAT and various amounts of pCMVhGRβ (Fig. 9*B*), the hGRα-mediated stimulation of CAT expression is inhibited in a dose-dependent manner, and the repression of hGRα activity is similar to that observed on the MMTV promoter. The inhibitory action of hGRβ is restricted to glucocorticoid-responsive promoters because the hGRβ protein has no effect on the constitutively active, nonglucocorticoid-responsive thymidine kinase CAT reporter plasmid (pBLCAT2) (data not shown). In sum, these results suggest that hGRβ represses the function of hGRα by specifically inhibiting GRE-mediated transcription.

DISCUSSION

Alternative splicing of the hGR primary transcript produces two highly homologous isoforms, termed hGRα and hGRβ, which differ at their carboxyl termini (1, 2). In contrast to the well characterized hGRα isoform, very little is known about the hGRβ splice variant. In this report, we examine the expression, biochemical properties, and physiological function of hGRβ. Northern blot analysis with a hGRβ-specific riboprobe demonstrates the presence of a message approximately 4.3 kb in size (consistent with the length of the hGRβ cDNA) in many different human tissues. We subsequently confirmed by RT-PCR that the alternative splicing event proposed to underlie the formation of the hGRβ mRNA transcript occurs in these tissues as well as in several transformed human cell lines. Together, these results indicate that the hGRβ message is endogenous to a variety of cells. Because both the hGRα and hGRβ messages are co-expressed in many of the same tissues, previous studies investigating hGRα expression with probes that did not discriminate between hGRα and hGRβ may be in error. The hGRβ mRNA transcript generated *in vivo* from the pCMVhGRβ expression vector is efficiently translated into the 90-kDa hGRβ protein in transfected COS-1, CV-1, and HeLa S_3 cells, suggest-

ing that the endogenous hGRβ message can also serve as a template for protein synthesis. However, whether the endogenous hGRβ message is actually translated into the hGRβ isoform is unknown. Anti-hGR antibodies made to date in several different laboratories have epitopes in the amino terminus and thus recognize both the hGRα and hGRβ proteins. The small difference in size between the two isoforms and the potential for hGRα to be post-translationally modified or degraded into a smaller protein make this cross-reactivity undesirable. To test directly for the expression of the hGRβ protein, we are presently making a hGRβ-specific antibody.

During our investigation of the expression of the hGRβ message, we made several observations that provide new insights both into the structure of the hGR gene and hGRα mRNAs and into the expression of the hGRα messages. The hGR gene has been previously reported to consist of 10 exons (2). Results from our Northern blot and RT-PCR analyses suggest that the last two exons, 9α and 9β, and the intronic sequences separating these two exons (intron J) together form one large terminal exon (exon 9). Exon 9 encodes the 3′ end of the hormone-binding domain of the hGRα protein (under normal splicing conditions) and contains approximately 4.0 kb of 3′UTR. It is interesting to note that the genes for the human androgen receptor, human estrogen receptor, and chicken progesterone receptor show a similar organization to that we have proposed here for the hGR. In each case, the most 3′ exon (exon 8) encodes the COOH-terminal portion of the hormone-binding domain and specifies a very large 3′UTR (38–42). The differential hybridization of the hGRα- and hGRβ-specific riboprobes with the 7.0- and 5.5-kb hGRα messages suggests that they originate from the use of alternative polyadenylation signals located in the 4.0-kb 3′UTR of exon 9. Similar alternative polyadenylation events have been proposed to explain the GR mRNA heterogeneity observed in rat tissues (35). Within the 3′UTR of eukaryotic mRNA reside signals that influence mRNA localization, mRNA stability, and translation initiation (43, 44). The 7.0- and 5.5-kb hGRα messages may differ in one or more of these properties. Both hGRα messages have a widespread tissue distribution, although the 5.5-kb hGRα message does not appear to be expressed at high levels in the brain. In addition, the 7.0-kb message is consistently more abundant than the 5.5-kb message.

The 7.0- and 5.5-kb hGRα messages are much more abundant than the 4.3-kb hGRβ mRNA transcript. Quantitative RT-PCR analysis of RNA isolated from two adult tissues and two human cell lines suggests that there is 200–500-fold more hGRα. However, because alternative splicing is often regulated in a spatial and/or temporal fashion, the hGRβ message may be expressed at higher levels in a tissue-specific and/or developmental stage-specific manner. In addition, the hGRα/hGRβ mRNA ratio may or may not reflect the hGRα/hGRβ protein ratio due to potential differences in stability and/or translation efficiency of the hGRα and hGRβ messages and/or due to differences in protein half-life. Furthermore, because the 7.0-kb hGRα message has the 9β sequences at its far 3′UTR, we cannot exclude the possibility that it also encodes the hGRβ protein. Development of hGRα- and hGRβ-specific antibodies will provide insight into this issue. Interestingly, the 9β sequences are well conserved in the rat GR cDNA 3′UTR, suggesting that an hGRβ homolog may exist in rat. RT-PCR analysis of rat liver (as well as a mouse lymphoma cell line) does indeed produce a PCR product that comigrates with the 366-bp PCR fragment derived from human cells.[2] Thus, although the hGRβ message is expressed at low levels relative to the hGRα mRNA transcripts in the human tissues so far examined, its conservation across species suggests that it plays an important physiological role.

With few exceptions (45, 46), modification of the GR hormone-binding domain results in a reduction or complete loss of hormone binding (3, 47–50). The COOH-terminal 50 amino acids of hGRα have been replaced in hGRβ with 15 unique amino acids. In agreement with previous reports (1, 3, 17), we show that this natural COOH-terminal modification prevents agonist binding to the hGRβ protein. Recently, it was reported that a truncated version of the human progesterone receptor B form missing the COOH-terminal 42 amino acids did not bind progesterone or the synthetic agonist R5020 but still bound the antiprogestin RU486 (51). This finding suggested that amino acids at the extreme COOH terminus of the human progesterone receptor are critical for agonist but not antagonist binding. Because members of the steroid hormone receptor superfamily share many of the same properties, we tested the ability of hGRβ to bind RU486 but found no evidence of binding. The 15 amino acids at the end of hGRβ may prevent the association of RU486 with this isoform. Alternatively, the observation made for human progesterone receptor B form may not be conserved among other family members. At this time, hGRβ is more aptly described as an orphan receptor whose natural ligand, if any, is unknown.

The hGRα receptor isoform translocates from the cytoplasm to the nucleus in a hormone-dependent manner (11). In the absence of hormone, the association of hsp90 with hGRα appears to inactivate the NLS (52, 53). Once hormone binds hGRα, hsp90 dissociates from the receptor resulting in the activation of the NLS and subsequent nuclear import of hGRα (8). In contrast to hGRα, we demonstrate that hGRβ resides primarily in the nucleus of transfected cells independent of hormone treatment. The amino acids necessary for interacting with hsp90 (7) are present in hGRβ, suggesting that hGRβ may be in the nucleus in spite of its association with hsp90. Perhaps the unique COOH-terminal amino acids of hGRβ delete sequences that inhibit the NLS or slightly alter the tertiary structure of the hGRβ/hsp90 complex such that the NLS are partially activated. This might account for our observation that most, but not all, of the hGRβ protein is located in the nucleus. Further studies will be required to elucidate the precise mechanism(s) underlying the nuclear distribution of hGRβ.

In the absence of hGRα, the hGRβ isoform is transcriptionally inactive on the MMTV enhancer independent of steroid treatment. However, when hGRα and hGRβ are expressed in the same cell, hGRβ inhibits the glucocorticoid-induced, hGRα-mediated activation of the MMTV promoter. Although this dominant negative effect was first reported in COS-7 cells cotransfected with hGRα and hGRβ expression vectors (17), we have extended this initial observation in several respects. First, we demonstrate that this dominant negative activity occurs in cells that have endogenous hGRα receptors. In addition, we show that the repression of hGRα activity occurs with the simple promoter pGRE2CAT. This indicates that the repression is a general phenomenon of glucocorticoid-responsive promoters and that it is GRE-mediated transcription that is actually inhibited.

The mechanisms responsible for the hGRβ-mediated repression of hGRα activity are unknown. The hGRβ protein is primarily located in the nucleus of transfected cells, has an intact DNA-binding domain and has been reported to bind a consensus GRE *in vitro* (17). Therefore, it may compete with hGRα for binding to the GRE. Another possibility is that hGRβ forms a heterodimer with hGRα that is transcriptionally inactive or less active than an hGRα homodimer. Alternatively, the hGRβ isoform may inhibit the function of hGRα by interacting with and titrating out an essential cofactor needed by hGRα for full

transcriptional activity. We are currently trying to identify the mechanism(s) responsible for the dominant negative activity of hGRβ and to determine whether hGRβ can inhibit hGRα-mediated repression of gene expression. Moreover, we hope to discern if hGRβ exhibits its dominant repressive effect on other members of the closely related subgroup of nuclear receptors that includes the progesterone, androgen, and mineralocorticoid receptors.

We have demonstrated that an alternatively spliced form of the hGR is present in many different tissues and is able to antagonize the physiological function of its predominant gene product. Alternative splicing plays a critical role in regulating the activity of several other members of the steroid/thyroid/retinoic acid receptor superfamily. Most closely resembling that observed for hGRα and hGRβ is the processing that occurs at the thyroid hormone receptor α subunit (TRα) locus. Alternative splicing of the last exon generates two receptor isoforms, TRα1 and TRα2, that differ at the carboxyl terminus (36). The TRα2 isoform does not bind thyroid hormones, but it represses the transcriptional activity of TRα1 by competing with TRα1 for binding to the thyroid hormone receptor responsive elements (36). Clearly, the ability of steroid/thyroid/retinoic acid receptor genes to encode transcription factors with opposing biological activities adds another level of complexity to the regulation of the function of these receptors.

Acknowledgments—We thank Dr. Ron Evans for the hGR clones OB7 and OB10 and Dr. Darryl Zeldin for human liver and lung total RNA. We also appreciate the technical assistance of Roger Componovo.

REFERENCES

1. Hollenberg, S. M., Weinberger, C., Ong, E. S., Cerelli, G., Oro, A., Lebo, R., Thompson, E. B., Rosenfeld, M. G., and Evans, R. M. (1985) *Nature* **318,** 635–641
2. Encio, I. J., and Detera-Wadleigh, S. D. (1991) *J. Biol. Chem.* **266,** 7182–7188
3. Giguere, V., Hollenberg, S. M., Rosenfeld, M. G., and Evans, R. M. (1986) *Cell* **46,** 645–652
4. Evans, R. M. (1988) *Science* **240,** 889–895
5. Carson-Jurica, M. A., Schrader, W. T., and O'Malley, B. W. (1990) *Endocr. Rev.* **11,** 201–220
6. Yamamoto, K. R. (1985) *Annu. Rev. Genet.* **19,** 209–252
7. Dalman, F. C., Scherrer, L. C., Taylor, L. P., Akil, H., and Pratt, W. B. (1991) *J. Biol. Chem.* **266**, 3482–3490
8. Picard, D., and Yamamoto, K. R. (1987) *EMBO J.* **6,** 3333–3340
9. Dahlman-Wright, K., Wright, A. P. H., and Gustafsson, J.-A. (1992) *Biochemistry* **31,** 9040–9044
10. Hollenberg, S. M., and Evans, R. M. (1988) *Cell* **55,** 899–906
11. Webster, J. C., Jewell, C. M., Sar, M., and Cidlowski, J. A. (1994) *Endocr. J.* **2,** 967–969
12. Pratt, W. B. (1993) *J. Biol. Chem.* **268,** 21455–21458
13. Jonat, G., Rahmsdorf, H. J., Park, K. K., Cato, A. C., Gebel, S., Ponta, H., and Herrlich, P. (1990) *Cell* **62,** 1189–1204
14. Yang Yen, H. F., Chambard, J. C., Sun, Y. L., Smeal, T., Schmidt, T. J., Drouin, J., and Karin, M. (1990) *Cell* **62,** 1205–1215
15. Schule, R., Rangarajan, P., Kliewer, S., Ransone, L. J., Bolado, J., Yang, N., Verma, I. M., and Evans, R. M. (1990) *Cell* **62,** 1217–1226
16. Scheinman, R. I., Gualberto, A., Jewell, C. M., Cidlowski, J. A., and Baldwin, A. S. (1995) *Mol. Cell. Biol.* **15,** 943–953
17. Bamberger, C. M., Bamberger, A.-M., de Castro, M., and Chrousos, G. P. (1995) *J. Clin. Invest.* **95**, 2435–2441
18. Andersson, S., Davis, D. L., Dahlback, H., Jornvall, H., and Russell, D. W. (1989) *J. Biol. Chem.* **264**, 8222–8229
19. DeFranco, D., and Yamamoto, K. R. (1986) *Mol. Cell. Biol.* **6,** 993-1001
20. Allgood, V. E., Oakley, R. H., and Cidlowski, J. A. (1993) *J. Biol. Chem.* **268,** 20870–20876
21. Luckow, B., and Schutz, G. (1987) *Nucleic Acids Res.* **15,** 5490
22. Allgood, V. E., Powell-Oliver, F. E., and Cidlowski, J. A. (1990) *J. Biol. Chem.* **265,** 12424–12433
23. Burnstein, K. L., Jewell, C. M., Sar, M., and Cidlowski, J. A. (1994) *Mol. Endocrinol.* **8,** 1764–1773
24. Tully, D. B., and Cidlowski, J. A. (1989) *Biochemistry* **28,** 1968–1975
25. Cidlowski, J. A., Bellingham, D. L., Powell-Oliver, F. E., Lubahn, D. B., and Sar, M. (1990) *Mol. Endocrinol.* **4,** 1427–1437
26. Sompayrac, L. M., and Danna, K. J. (1981) *Proc. Natl. Acad. Sci. U. S. A.* **78,** 7575–7578
27. Gorman, C. (1985) *DNA Cloning: A Practical Approach* (Glover, D. M., ed) Vol. 3, pp. 143–190, IRL Press, Oxford
28. Rosewicz, S., McDonald, A. R., Maddux, B. A., Goldfine, I. D., Miesfeld, R. L., and Logsdon, C. D. (1988) *J. Biol. Chem.* **263,** 2581–2584
29. Brandon, D. D., Markwick, A. J., Chrousos, G. P., and Loriaux, D. L. (1989) *Cancer Res.* **49,** (suppl.) 2203–2213
30. Bronnegard, M., Werner, S., and Gustafsson, J.-A. (1991) *J. Steroid Biochem. Mol. Biol.* **39,** 693–701
31. Domin, W. S., Chait, A., and Deeb, S. S. (1991) *Biochemistry* **30,** 2570–2574
32. Zeiner, M., and Gehring, U. (1993) *Cancer Res.* **53,** 3513–3517
33. Denton, R. R., Eisen, L. P., Elsasser, M. S., and Harmon, J. M. (1993) *Endocrinology* **133,** 248–256
34. Devereux, J., Haeberli, P., and Smithies, O. (1984) *Nucleic Acids Res.* **12,** 387–395
35. Miesfeld, R., Rusconi, S., Godowski, P. J., Maler, B. A., Okret, S., Wikstrom, A.-C., Gustafsson, J.-A., and Yamamoto, K. R. (1986) *Cell* **46,** 389–399
36. Koenig, R. J., Lazar, M. A., Hodin, R. A., Brent, G. A., Larsen, P. R., Chin, W. W., and Moore, D. (1989) *Nature* **337,** 659–661
37. Meyer, M.-E., Pornon, A., Ji, J., Bocquel, M.-T., Chambon, P., and Gronemeyer, H. (1990) *EMBO J.* **9,** 3923–3930
38. Kuiper, G. G. J. M., Faber, P. W., van Rooij, H. C. J., van der Korput, J. A. G. M., Ris-Stalpers, C., Klaassen, P., Trapman, J., and Brinkmann, A. O. (1989) *J. Mol. Endocrinol.* **2,** R1–R4
39. Faber, P. W., van Rooij, H. C. J., van der Korput, H. A. G. M., Baarends, W. M., Brinkmann, A. O., Grootegoed, J. A., and Trapman, J. (1991) *J. Biol. Chem.* **266,** 10743–10749
40. Green, S., Walter, P., Kumar, V., Krust, A., Bornert, J.-M., Argos, P., and Chambon, P. (1986) *Nature* **320,** 134–139
41. Ponglikitmongkol, M., Green, S., and Chambon, P. (1988) *EMBO J.* **7,** 3385–3388
42. Jeltsch, J.-M., Turcotte, B., Garnier, J.-M., Lerouge, T., Krozowski, Z., Gronemeyer, H., and Chambon, P. (1990) *J. Biol. Chem.* **265,** 3967–3974
43. Jackson, R. J., and Standart, N. (1990) *Cell* **62,** 15–24
44. Jackson, R. J. (1993) *Cell* **74,** 9–14
45. Chakraborti, P. K., Garabedian, M. J., Yamamoto, K. R., and Simons, S. S., Jr. (1991) *J. Biol. Chem.* **266**, 22075–22078
46. Warriar, N., Yu, C., Govindan, M. V. (1994) *J. Biol. Chem.* **269,** 29010–29015
47. Rusconi, S., and Yamamoto, K. R. (1987) *EMBO J.* **6,** 1309–1315
48. Danielsen, M., Northrop, J. P., and Ringold, G. M. (1986) *EMBO J.* **5,** 2513–2522
49. Hollenberg, S. M., Giguere, V., and Evans, R. M. (1989) *Cancer Res.* **49,** (suppl.) 2292–2294
50. Hurley, D. M., Accili, D., Stratakis, C. A., Karl, M., Vamvakopoulos, N., Rorer, E., Constantine, K., Taylor, S. I., and Chrousos, G. P. (1991) *J. Clin. Invest.* **87,** 680–686
51. Vegeto, E., Allan, G. F., Schrader, W. T., Tsai, M.-J., McDonnell, D. P., and O'Malley, B. W. (1992) *Cell* **69,** 703–713
52. Picard, D., Salser, S. J., and Yamamoto, K. R. (1988) *Cell* **54,** 1073–1080
53. Scherrer, L. C., Picard, D., Massa, E., Harmon, J. M., Simons, S. S., Yamamoto, K. R., and Pratt, W. B. (1993) *Biochemistry* **32,** 5381–5386